Torture, 2025, 35(1), 26-37
https://doi.org/10.7146/torture.v35i1.150054 *Research Paper*

Recovery and study of human remains at the Chapel of S. Domenico – Al-Tahira Cathedral, Iraq: Medico-legal and forensic anthropological investigations

Laura Donato[1, 2], Douglas H Ubelaker[3, 2], Rossana Cecchi[4], Jessika Camatti[5], Marco Albore[6], Gianpiero D'Antonio[6], Gabriele Napoletano[6], Letizia Sorace[6], Michele Treglia[7,2], Luigi Tonino Marsella[7, 2] and Costantino Ciallella[6]

1 PhD program in Applied Medical Surgical Sciences, Department of Surgical Sciences, University of Tor Vergata, Rome (Italy).
2 Laif (laboratorio di Antropologia e Invecchiamento Forense), Sezione di medicina legale, sicurezza sociale e tossicologia forense, University of Tor Vergata, Rome (Italy).
3 Smithsonian Institution, Washington, DC, USA.
4 University of Modena and Reggio Emilia, Modena (Italy).
5 University of Parma, Parma (Italy). Correspondence to: jessikacamatti@gmail.com
6 Department of Anatomical, Histological, Forensic and Orthopedic Sciences, Sapienza University of Rome, Rome
7 Department of Surgical Sciences, University of Tor Vergata, Rome

Key points of interest:

- Contemporary forensic anthropological investigations can be applied to the study of torture allegations in historical cases.

Abstract

Introduction: The Chapel of St. Dominic of the Cathedral of 'Al-Tahira' in Qaraqosh (Iraq) allegedly contained human remains belonging to two victims, according to the testimonies of locals. In this article, the authors discuss the recovery and study of human remains that took place there in May 2022. *Methods:* Italian forensic anthropologists and pathologists conducted excavations, discovering skeletal remains identified as two individuals (C1 and C2). Bones were analysed for sex, age, height, and dental traits, and underwent microscopic examination. Anatomically repositioned remains were scanned via CT, and facial reconstructions were made. The cause and manner of death were hypothesised. *Results:* An extensive fracture complex with transverse orientation was observed in the occipital region of C1. C2 showed cranial disintegration, with fracture fragments affecting the structures of the left neuro- and splanchnic skull, and to a greater extent, the left hemifacial, orbital, and zygomatic regions and the same side of the face. In addition, no bones attributable to the left hand of C2 were found. *Discussion:* Concerning C1, nothing precludes that the death occurred due to severe blunt-fracture trauma with greater expression at the level of the cranial district. On the other hand, it seems reasonable to assume that C2 was the victim of an assault in which his left hand was amputated, he was beaten and pierced by a bayonet, and finally, he was killed with a rifle shot to the head.

Keywords: human remains, buried human bodies, forensic anthropology, human bones, forensic science

Introduction

In cases of buried human bodies, the assessment first aims to analyse the modalities of burial in the ground and, therefore, involves areas that are not directly referable to the biological sciences of the study of the corpse.

Thus, this part of the investigation is essentially carried out in situ and continues, in continuity of operations, by analysing how the human remains were found, examining their position and any alterations to their integrity, which can also be attributed to geological variations in the terrain.

The next phase concerns the extraction of the bone remains from the burial and their observation, as well as re-aggregating them to form the original skeleton. This phase involves recovering the integrity of the skeletal segment in its anatomical form and observing the possible presence of alterations to the original form that may suggest information relating to the age of the subject at death, their stature, the manner of death and other elements (White & Folkens, 2005; Christensen et al., 2019; Klepinger, 2006).

The Chapel of St. Dominic of the Cathedral of 'Al-Tahira' in Qaraqosh (Iraq) allegedly contained human remains belonging to two victims, according to the testimonies of locals.

According to testimonies, in June 1915, two Christian priests travelled from Mosul to Bakhdida (Qaraqosh) with four merchants after visiting the bishop. Following a recent Ottoman military defeat and the killing of a soldier in Qaraqosh, the merchants fled while the priests continued. Ottoman soldiers intercepted the priests, and while the 33-year-old initially escaped, the 44-year-old was likely shot. Witnesses report that when the younger priest returned, he was subjected to torture, including amputation of his left hand, and was ultimately killed by a cut to the throat.

This paper discusses the recovery and study of human remains at the Chapel of S. Domenico – Al-Tahira Cathedral of the Syro-Catholic Archdiocese of Mosul, located in Qaraqosh, Iraq, which took place in May 2022.

Materials and methods

In May 2022 at the request of the Postulator of the Causes of Saints, Rev. Dr. Luis Fernando Escalante, with a mandate conferred by the *Congregatio de causis sanctorum*, Vatican City, a search began for two bodies allegedly belonging to two individuals, according to the testimonies of locals, in the Chapel of St. Dominic of the Cathedral of "Al - Tahira" in Qaraqosh (Iraq). The excavations took place inside the Chapel, in an area in front and to the right of the altar, near an epigraph on the wall of the east-facing side of the chapel, and involved a multidisciplinary working team from Rome, which included five forensic pathologists and one forensic anthropologist.

After a prolonged excavation, skeletal remains of two individuals were uncovered in a tomb structure made of bricks and mortar. Located about 1.86 m below floor level, the tomb was reached by removing layers of marble-granite, cement, earth, and a final brick layer, likely part of the hypogeum vault. The tomb, parallel to the altar, was oval-shaped with a west-east orientation for the central axis and south-north for the transverse axis. The remains were positioned with their bodies oriented west-east. Henceforth, they were identified by the abbreviations C1 and C2 (Figure 1). Fragments of emerald, green fabric, likely ecclesiastical burial clothing, were found on both individuals. Ornamental vessels, approximately 1 cm in diameter and discoidal in shape, were found on the right side of each skull.

***Figure 1**: The left photo illustrates the cleaning of the skeletal remains using soft brushes during the excavation phase; referring to the central image, C1 is located on the left, while C2 is on the right. The right photo better visualises the position of the ornamental vessels concerning the skeletal remains.*

The forensic anthropologist examined each bone, also inferring information about sex determination, height calculation, age at death calculation, and dental formula. Bone elements also underwent microscopic examination. Both anatomically repositioned bone remains were subjected to CT examination, and facial reconstructions of the two examined individuals were performed. Finally, the cause and manner of death of C1 and C2 were hypothesised based on the multidisciplinary investigations conducted.

Results

a. Forensic anthropology investigations: Study of individual C1

a.1 Revision of bone remains

– Skull: An extensive fracture complex with transverse orientation is observed in the occipital region (Figure 2).

The equatorial fracture line is divided into two sections by the sagittal suture. The first extends leftward for 2.5 cm before branching into three lines. The second moves supero-externally for 1.5 cm, orthogonal to the first and superior by 2 cm. The third moves infero-externally for 3 cm to the left of the lambdoid suture. The right line extends 3 cm rightward before branching infero-externally to rejoin the left lambdoid suture. The first branch extends supero-externally for 7 cm, branching into two 1 cm arms. The second extends laterally for 3 cm, and the third moves inferiorly to rejoin the right lambdoid suture. The mandible shows a weak connection to the splanchnocranium.

Figure 2. *C1, skull: extensive fracture complex in the occipital region.*

Ribs: The fracture of the 5th right rib is reported.

Vertebrae: Nothing to report.

– Right scapula: scapular plate with two longitudinal fractures, parallel to each other, converging approximately in the centre at the level of the right fourth rib, from anterior to posterior.
– Left scapula: Nothing to report.
– Pelvis: Fracture of the left innominate.
– Humerus: The head crest is more accentuated to the left.
– Radius: The distal epiphysis of the right radius is slightly larger than that of the left radius.
– Right and left ulna: Nothing to report.
– Right hand: Nothing to report.
– Femur: the angle of bony prominence in the area where the distal epiphysis articulates with the patella is also present bilaterally, but externally on the right is less developed than on the left. On the left: slight protrusion at the level of the inner margin of the epiphysis; pitting at the level of the condyle internally.
– Right and left patella: Nothing to report.
– Right and left tibia: In the proximal region, slight pitting is present.

a.2 Sex determination

Masculine character (glabella +1, mastoid process +2, supraorbital margin +2, occipital protuberance +1, mandible +1, chin +1, mandibular angle +1, inferior margin +1, upright ramus+1, mandibular condyle +1, posterior margin upright ramus+2) (Acsádi & Nemeskéri, 1970).

a.3 Height calculation

– Measurements for determining the height: right humerus length: 33.0 cm; right ulna length: 27.3 cm; right radio length: 25cm; right femur length: 47 cm; right tibia length: 37 cm; right fibula length: 36.5 cm; left humerus length: 33 cm; left ulna length: 27.5 cm; left radio length: 23.5cm; left femur length: 45.5 cm (broken); left tibia length: 37.6 cm; left fibula length: 36.5 cm.
– Height calculation (Trotter, 1970; Lee et al, 2024)

White males (18-30 years old). 1.30 (Fem + Tib) + 63.29 +- 2.99

1.30 (47 + 37) + 63.29 +-2.99 = 172 +- 2.99 cm (range 169.5 – 175.48 cm).

a.4 Calculating Age at Death (Ost, 2022; Lovejoy et al., 1985)

Stage 5: Partial densification of the auricular surface, moderate retroauricular activity, and slight alteration (osteophytes) are possible at the surface's apex (lower margin). Age 40-44 years.

a.5 Dental formula

Right maxilla: teeth C^1 to M^2 present in situ; presence of ceramic prostheses with a triangular base and scalloped edges; the base measures 3.5 cm and the height is 2.5 cm and has a concavity that recalls the anatomy of the upper palate; the end of this prosthesis is modelled in ceramic in the shape of an incisor which, in the overall arrangement of the elements, corresponds to I^1. Left maxilla: present in situ from C^1 to M^2; the remaining elements are absent. Right mandible: M_3 present not in situ; M_2, M_1, P_3 present in situ; P_4 present not in situ; C_1, I_2, I_1 present in situ. Left mandible: M_3, M_2, M_1, P_3, P_4, C_1, I_2, I_1 present in situ.

b. Forensic anthropology investigations: Study of individual C2

b.1 Revision of bone remains2

– Skull (Figure 3): presence of cranial disintegration with fracture fragments affecting the structures of the left neuro- and splanchnic skull and to a greater extent the left hemifacial, orbital, zygomatic regions and the same side of the face. In the left temporo-parietal-occipital region, there is a large area of substance loss with an extensive comminuted fracture, loss of the typical conformation of the cranial ovoid, and partial dispersion of the fragments. Seven fragments are in the immediate vicinity due to the interposition of earthy material.

  A curvilinear fracture originates medially in the left orbit, crossing the glabella obliquely from left to right and moving upward into the right frontal region with leftward concavity.

  In the middle third, the first fracture branches transversely 1 cm to the right, while the main fracture continues to 2 cm from the coronal suture.

  In the temporal region, anterior to the extensive area of bone loss, two linear fractures are present: one oblique from inferior-superior to posterior-anterior, ending in the left frontal region, and another one with an almost vertical course from inferior to superior, lateral to medial, terminating in a rounded, irregular-looking area in the left parietal region.

  Our manual reconstruction of the left temporo-parietal-occipital region was incomplete due to persistent fragment loss, particularly in the postero-lateral area. The defect primarily involves the occipital squama, trapezoidal in shape, with a lateral major side and a medial minor side. The smaller side reveals a roughly rounded laceration (1.2 cm in diameter), uniformly coloured with the surrounding bone. Margins show inward flaring extending 2 cm, visible along the internal cranial table. This is highlighted with a red line in the image, with margins showing flaring of the walls on the internal cranial table.

  A fragment of rusty metal with a length of 4.3 cm is found in the middle and posterior cranial fossa. The left facial region is altered by the absence of the maxilla and zygomatic bone, and fractures are observed in the mandible at the right horizontal ramus level. At the same time, on the left, there is substance loss at the mandibular angle level.
– Sternum and clavicles: nothing to report.
– Right rib cage: at the level of the 4th rib, there is a complete fracture of the rib body (Figure 4); on the vertebral end of the 5th rib, in correspondence with the joint with the vertebral apophysis, there is a sulcus of suspected nature
– Left rib cage: fracture of the 3rd rib. -
– Vertebrae: lesion of the L5 vertebral body, which extends throughout the volume from top to bottom, keeping the vertebral body connected
– Right scapula (Figure 5): Fragmented into four sections in the acromion and proximal aspects. At the level of the scapular

Figure 3. *C2, skull.*

Figure 4*. C2; the fourth right rib is fractured on the left side of the photo.*

plateau, two full-thickness lacerations of bone tissue are detected. Their margins appear everted in a posterior direction from front to back, which are referred to as lesion A (inferior) and lesion B (superior).

Lesion A is located in the distal third, in correspondence with the medial side of the scapula. It has a triangular shape and a greater transversal axis, with an acute angle facing the lateral profile of the scapula. The base of this lesion is almost parallel to the medial profile of the bone. It has a length of approximately 0.60 cm and a width at the base of approximately 0.25 cm, with sharp margins. A thin, irregular fracture originates from the corner of this lesion, which moves obliquely from inferior to superior and from medial to lateral for about 2 cm.

Figure 5. *C2, right scapula.*

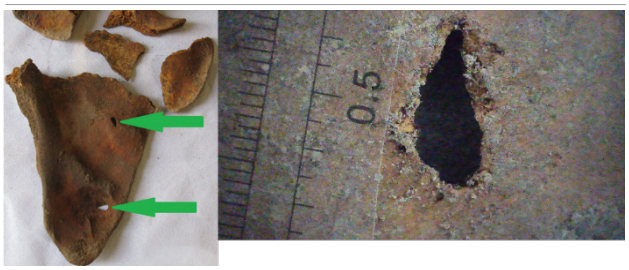

Lesion B is in the middle third of the bone, near its medial side. It has a triangular shape, a central oblique axis from top to bottom, and an altered-medial direction, with an angle slightly turned towards the medial and near scapular margin to the upper edge of the scapula. It is approximately 0.6 cm long and approximately 0.3 cm wide at the base. Macroscopically, almost clean margins characterise it.

- Left scapula: Fragmentation of the proximal area into three sections. It presents a laceration piercing the bone tissue at the level of the middle third of the medial margin. It shows a right angle in the lateral direction and two slightly indented margins in the medial direction.
- Right innominate: Fragmented and with loss of its anatomical continuity. Absence of the ventral arch, indicative of male sex, is observed. The articular surface of the symphysis pubis is smooth. The trend is regular both in terms of area and perimeter. Acetabular cavity halved.
- Left innominate: Fragmented, with large fragments. Absence of ventral arch.
- Sacrum: Fragmented in its proximal posterior position.
- Right humerus: The presence of numerous fissures from fracture is noted.
- Right radius: Fragmented with slight pitting at the distal epiphysis. The proximal epiphysis is also absent; the fracture line has a whitish colour, where it is fragmented, but as it proceeds inwards, it tends to take on a homogeneous colour to the surrounding bone tissue.
- Right ulna: Fracture near the proximal metaphysis and slight hyperostosis near the olecranon, more severe than the opposite one. Slight prominence in the inferior region of the olecranon joint.
- Right hand: Nothing to report.
- Left humerus: Fractures that extend along the entire length of the diaphysis. The fracture had a homogeneous colour compatible with pressure movements from case failure and fractures of the condyles of light colour. Posteriorly, there is an accentuated crest at the level of the humeral head.
- Left ulna: Interrupted in continuity at the proximal metaphysis and the distal third level. The distal epiphysis presents a fracture of the tip of the ulnar styloid and fractures along the entire diaphysis of homogeneous colour. At the level of the proximal epiphysis, slight hyperostosis of the olecranon joint is observed.
- Left radius: Interrupted in its continuity in the middle third in the absence of the head. Fracture lines running along the length of the diaphysis are evident. A chromatic difference of the fracture present at this level can be appreciated near the distal epiphysis.
- Right femur: Usually shaped and intact. The posterior aspect of the head has cam deformities with slight thickening of the edges. The linea aspera is less marked on the right side than on the left, with slight weakening of the bony structure of the proximal epiphysis.

  The distal epiphysis is affected by posterior pitting with characteristics like the opposite ones.
- Right patella: Usually shaped and intact, with a more robust and rounded shape than the left one.
- Right tibia: Fragmentation of the proximal epiphysis and partial loss of the posterior cortical surface with hypochromic fracture margins. The distal epiphysis has less marked bone development than the corresponding opposite region, with slight pitting of the other facet joints.
- Right fibula: Eversion of the cortical surface of the distal epiphysis with pitting.
- Right foot: Calcaneal enthesis is more developed than the opposite one; it is jagged and robust in appearance but with fewer vertical striae and bony protrusions indicative of great-

er flexion (different traction). Pitting present at the level of the talus with slight relief of the facet joints.
- Left femur: Usually shaped and intact. A cam deformity is present on the posterior aspect of the head. Posteriorly, the bone has a well-developed rough line. In the posterior region, pitting is present between the two condyles of the distal epiphysis. At the level of the distal epiphysis, both internally and externally, there is a slight elevation of the crest that extends up to the posterior facets,
- Left patella: anteriorly striations and furrows, as from the excavation of tendons on the bone (enthesis). Posteriorly, a slight elevation of the facet and bone crest. The left aspect has a flatter and more tapered shape than the right.
- Left tibia: pitting at the level of the anterior aspect of the proximal epiphysis. Bone crest in the anterior part of the upper tibial epiphysis. Protrusion of the line on the posterior articular surface facing inward. The anterior region of the shaft and proximal tibial epiphysis are well developed. The distal epiphyses show a protrusion of the posterior line with the squatting facet and protrusion of the posterior articular face of the tibia at the level of the proximal epiphysis.
- Left fibula: fracture of the distal epiphysis, which prevents a complete evaluation.
- Left foot: partially reconstructed, sesamoid bones were located. Moderately developed posterior calcaneal entheses, raised and striated surface, and underlying lower facets. Slight pitting of the talus, with slight development of the joint margins. There is slight pitting in the remaining bone elements of the tarsus examined.

b.2 Sex determination

Masculine character (marked glabella +1, extensive mastoid process +1, marked browbone +1, almost vertical upright ramus +1).

b.3 Height calculation

- Measurements for determining the height: right ulna length: 27.3 cm; right radio length: 24.8 cm; right femur length: 44.0 cm; right tibia length: 38.5 cm; right fibula length: 37.5 cm; left humerus length: 31 cm; left ulna length: about 27.8 cm; left radio length: 24.3 cm; left femur length: 44 cm (broken); left tibia length: 38 cm; left fibula length: 38 cm.
- Height calculation (Trotter, 1970; Lee et al, 2024)

  White males (18-30 years old). 1.30 (Fem + Tib) + 63.29 +- 2.99

  1.30 (44 + 38.5) + 63.29 +-2.99 = 170.54 +- 2.99 cm (range 167.55 – 173.53 cm).

b.4 Calculating age at death

Pubic symphysis modification (Baca et al, 2022; Todd, 1920) stage 6-7 (estimated age 30-35/39-44); sternal end fourth rib changes (Iscan, 2013) stage 3 (estimated age 25-34). Therefore, from the analysis of the available elements, it is possible to conclude that C2 had an estimated age between 25-39 years at the time of death.

b.5 Dental formula

Right maxilla: M^3 included. The remaining teeth are present in situ. Left maxilla: present in situ from C^1 to M^1; the remaining elements are absent. Right mandible: from M_3 to C_1 present in situ; I_2 present not in situ; I_1 absent. Left mandible: I_1, I_2 are not present in situ; the remaining teeth are in situ.

c. Medico-legal investigations

After a macroscopic study on site, after exhumation and recovery of the individual bones, a microscopic investigation was carried out with a Jiusion USB HD 2MP 40-1000X digital monocular microscope. This examination applied to C2 (4^{th} right rib, L5 vertebral body, scapulae, distal epiphysis of the ulna) revealed the presence of continuous full-thickness lesions, homogenously coloured to the outer bone covering, which can be identified with a high degree of probability as vital fractures attributable to the action of third parties. Lesion A of the right scapula showed slight irregularities, while slightly irregular margins characterised lesion B. The microscopic examination of the 5^{th} right rib of C2 documented the consolidation of a fracture.

Both anatomically repositioned bone remains were subjected to CT examination at the Saint Mary Medical Complex

Figure 6. *C1, 3D CT reconstruction of skull: fractures are visible in the right part of the skull.*

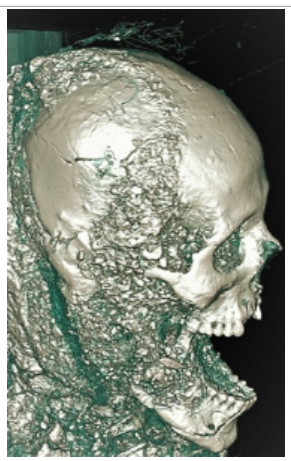

(SMC) diagnostic centre located in Qaraqosh, Mosul, to characterise better the lesions already found and exclude any alterations not visible macroscopically. Figure 6 shows the 3D CT reconstruction of the skull belonging to C1, which documents the fractures found macroscopically.

In addition, facial reconstructions of the two examined individuals were performed. This was done by acquiring CT scans of the skulls and then processing them using dedicated software to extrapolate their three-dimensional virtual volume from the DICOM file (Slicer 4.10.2). Then, the three-dimensional rendering of the skulls was manipulated using 3D graphics software (ZBrush, version 2022.0.6, Pixologic®). Using this software, it is possible to apply shims to the bone surface. These elements represent indicators of soft tissue thickness, the size of which varies depending on the sex, age at death and ethnicity of the individual examined. To this end, the biological profile was studied using a forensic anthropological method to obtain the necessary information. The application of the tissue shims preceded the processing of the facial physiognomy of the two individuals to get a characterisation of the physiognomic features (Figure 7). The accuracy of this technique has recently been the subject of a publication (Donato et al, 2024).

Discussion

The present paper discusses the discovery of the bone remains allegedly belonging to two Christian priests whose deaths were attributed to a violent traumatic event at the hands of third parties in 1915. At the time, Iraq was ruled by the Ottoman Empire, so Ottoman soldiers acted in that territory on behalf of that empire. According to the testimonies of local individuals, the reason why the priests were killed lay in the fact that they were individuals who belonged to the Christian religion and represented clerical exponents. In fact, in those days, the Ottoman convoy had suffered a military defeat in Mosul, and the day before, a soldier had been killed in Qaraqosh while attempting to rape a local Christian woman. For this reason, the moment the priests and merchants became aware of the presence of the Ottomans, the merchants ran for safety precisely because they feared that they were in danger as Christians. Unfortunately, the priests did not have the same perception of risk, and this cost them their lives.

In the present case, it seems clear that the discrimination of the subjects as openly belonging to Christian beliefs and as exponents of Christian beliefs at the community level constituted the *primum movens* of the violent event with a fatal outcome. The recent military defeat in Mosul and the recent

***Figure 7**. Facial reconstructions; on the top, left lateral, frontal, and right lateral views of C1's facial reconstruction; on the bottom, left lateral, frontal, and right lateral views of C2's facial reconstruction.*

killing of the soldier who had attempted to rape a Christian woman played a role in the decision to attack the two priests. Moreover, those who inflicted the violence held an official position concerning the Ottoman Empire that ruled Iraq in the year this event took place.

Consequently the facts could amount to torture with a final result of death.

It is likely, based on forensic and circumstantial data, that both deaths can be placed in a context of violent death for reasons of religious and ethical hatred.

Individual C1

C1 exhibited anthropological traits consistent with males aged between 40 and 44 years and an estimated height of 169.5–173.5 cm. Evidence of trauma included polyfractures predominantly affecting the posterior skull and brain, consistent with a blunt-fracture nature, likely resulting from a fall. Additional thoracic injuries (fractures of the right 5th rib and scapula) support this interpretation.

The study of skull fractures assumes relevance in the forensic context, especially to identify traumatogenesis. At the cranial level, five types of fractures can occur, namely: a) diffuse fracture complexes, b) circumscribed fracture complexes, c) isolated fractures of the cranial vault, d) fractures of the cranial vault radiating to the base, e) isolated fractures of the skull base.

In forensic analysis, cranial fractures are classified into five types: (a) diffuse complexes, (b) circumscribed complexes, (c) isolated vault fractures, (d) vault fractures radiating to the base, and (e) isolated basal fractures. These can result from direct trauma—either unipolar (localised impact) or bipolar (compression between opposing forces)—or indirect trauma, typically involving force transmission from distal body parts, as seen in ring fractures at the skull base.

Fracture patterns often follow meridian or equatorial orientations, depending on how traumatic forces stress or compress cranial diameters. This is due to the decrease in the diameter between the two points of application of the force or between the point of application and the reaction pole. It can depend on the increase in the perpendicular diameter, which induces a disintegration of the bone molecules by moving away from each other or tearing, resulting in fractures. If the force is particularly intense, the kneeling of the cranial case along the perpendicular diameter produces fracture lines that are arranged in an equatorial direction (Crudele et al., 2020, Haug et al., 1994; Simon & Newton, 2024; Yoganandan & Pintar, 2004, Sahoo et al, 2013, Sahoo et al, 2016).

Regarding the cranial fracture of C1 (Figure 2, Figure 6), such fractures are identifiable with an impact lesion on a large and wide surface. Therefore, this fracture complex can be considered as the result of a fall, or from being thrown from a horse, based on the harmful peculiarity and following the testimonial data collected on the spot and therefore to believe that the cause of death of C1.

In conclusion, there is reason to believe that death occurred due to severe contusion-fracture trauma with greater expression at the level of the cranial district and less expression at the thoracic level; as far as the means are concerned, they seem likely to be due to an impact against a rigid resulting from a fall from moderate height, possibly from a horse. The failure to highlight pathognomonic elements indicative of the action of a firearm against the cranial district does not allow for the confirmation of this harmful hypothesis.

Individual C2

C2 presented anthropological characteristics relating to the male sex, an estimated age at death between 25 and 44 years and an estimated height between 167.5 and 173.5 cm. Evidence of significant violence included extensive cranial trauma affecting the left splanchnocranium and neurocranium, thoraco-abdominal trauma (including a fractured right 4th rib and vertebral body at L5), and sharp force injuries to the right scapula. Notably, no bones attributable to the left hand were recovered, aligning with oral accounts of a possible amputation.

Compared to C1, C2 presented with more severe and extensive injuries. A significant cranial defect with loss of bone substance was observed, particularly on the left side, suggestive of high-energy trauma (Figure 3).

It therefore appears helpful in recalling some forensic pathological aspects of cranial firearm injuries. On a rigid surface, the entry into the bone shows a sharper and more linear margin at the level of the external table and a wider, flared hole on the internal table. The exit site is hollowed out in a truncated cone with the flaring facing outwards from the cranial cavity.

The production of secondary fractures of the skull depends on the firing distance and the projectile's kinetic energy. The gases produced by the shot contribute to the genesis of secondary fractures in shots fired on contact. In shots fired at long range, the secondary fractures are caused by the increase in pressure due to the direct effect of the projectile and by the phenomenon of the temporary cavity. Apart from other harmful factors, the greater the kinetic energy lost, the larger the temporary cavity, the pressure exerted on the braincase, and the extent of the secondary fractures. This can lead to an extensive and massive fracturing breakdown (Crudele et al., 2020; Haug et al., 1994; Simon & Newton, 2024; Yoganandan & Pintar, 2004; Sahoo et al, 2013; Sahoo et al, 2016).

Therefore, it is possible to state that a gunshot hit the head of C2. The lesion can be identified with a fractured area with collapse of the cranium compatible with the action of a projectile that penetrates and passes through the head.

Furthermore, secondary fractures, in the frontal and left parieto-temporal site, showed meridian and centrifugal direction associated with the loss of substance affecting the bones of the left hemiface. They are identifiable as a "burst" lesion.

Therefore, it is likely to believe that the massive lesion found in the cranial site may have caused the mortis of C2.

According to the witnesses, the two murders were attributed to a convoy of Ottoman troops. Moreover, it is possible to hypothesise that 1915-1917, MAUSER equipped the Ottomans with long-barrelled rifles. It was a German war rifle used during the First World War in the territories of the former Ottoman Empire and, therefore, also in Iraq (Ball, 2011).

Long-barrel shotguns can tolerate high pressure levels thanks to a more solid structure, and the barrel's length gives this type of weapon greater accuracy. The Mauser models support ammunition of 7.63 mm calibre, with a bullet mass of 5.5 g and a muzzle velocity of 430 m/s (Madea, 2014). Since the approximate estimates taken into consideration, it can be hypothesised that fractures affecting the left splanchnocranium and neurocranium are compatible with a fractured polytraumatic injury with greater cranial-brain expression resulting from the action of a long-barrelled gunshot.

A fragment of rusty metallic material was found in C2's skull. It was elongated, with a cocooned, pointed, and curved end. These elements do not allow us to attribute to the find any other genesis than that envisaged for the other metallic elements just mentioned.

Two continuous solutions passing through the bone tissue were in the right scapular plate. They showed margins everted posteriorly from front to back. They are named lesions A (lower) and B (upper). Each is approximately 0.6 cm long and identifiable as puncture wounds and cuts. Both are compatible with the action of a pointed and single-edged instrument.

The marks present at the level of the right scapula are compatible with the action of a tool equipped with a point, a wire and a rib. The weapon acted from front to back and had a length of at least 25 cm, i.e. such as to allow the penetration of the anterior region of the thorax and the penetration of the weapon up to the rear part of the rib cage, where the scapula is housed, piercing this last bone.

The alternative hypothesis, i.e. that of a bladed weapon struck behind individual 2, therefore from back to front, is incompatible with the dimensions of the two solutions found on the bone. Since the scapula is located immediately below the skin in correspondence with the dorsal region of the body, any blade that managed to cross it would have caused a larger imprint.

A length equal to 0.6 cm, if projected onto the blade of a commonly used knife, determines a penetration not exceeding one centimetre. Therefore, the blow delivered posteriorly would have been extremely superficial and, therefore, insufficient force to completely pierce a compact bone such as the scapula.

With this force, the weapon is positioned at the end of a lever and, therefore, acts by transferring and enhancing the violent energy the person holding the rifle applies.

The different orientations of the two figurative images observed on the scapula corroborate the proposed hypothesis. It suggests that driving the bayonet into the body of individual 2 was a rapid recurrence and a defensive action that involved a minimal shift in the position between aggressor and victim.

Considering the gunshot wound to the skull as a first lesion, there would have been an immediate incapacity of the victim with his fall to the ground.; In this static position, the insertion of the objects with the bayonet should have taken place with the imprint oriented in the same direction for both blows.

The weapon's different orientation supports the opposite hypothesis of a standing subject. In fact, after receiving the first blow, he makes an instinctive defence movement that retains a displacement of the weapon's central axis before the second inflexion.

Considering the analysed data, the chest may have been drawn from a bayonet.

About how the blade reached the chest, it is possible that the same blade mounted on the end of a rifle was used to pierce the chest, from front to back and from left to right.

The involvement of the right 5th rib, at the level of the anterior axillary line, is more probable due to its characteristics. It should also be noted that one of the two mould injuries at the level of the right scapula had a transversal central axis. The other was slightly oblique from lateral to medial, therefore compatible with the action of a sharp instrument that has crossed the intercostal spaces before drawing the scapula. For explanatory purposes only, some representations of the possible dynamics are given in Figure 8. Therefore, it seems reasonable that one or more subjects produced both the cranial-brain and thoracic lesions placed anteriorly concerning the victim.

The left-hand bones were associated with a transversal fracture of the ipsilateral ulnar styloid. The data support the testimonial hypothesis of its amputation during the lethal trauma dynamics. Almost all the bone structures of the hand were found in anatomical continuity with each other, although dis-

Figure 8. *Top left: Anterior view showing the entry point of a sharp, pointed instrument with a cutting edge. Top right: Posterior view illustrating the same type of instrument penetrating the scapula. Bottom: Lateral view depicting the trajectory of the sharp instrument as it enters the scapula from the side.*

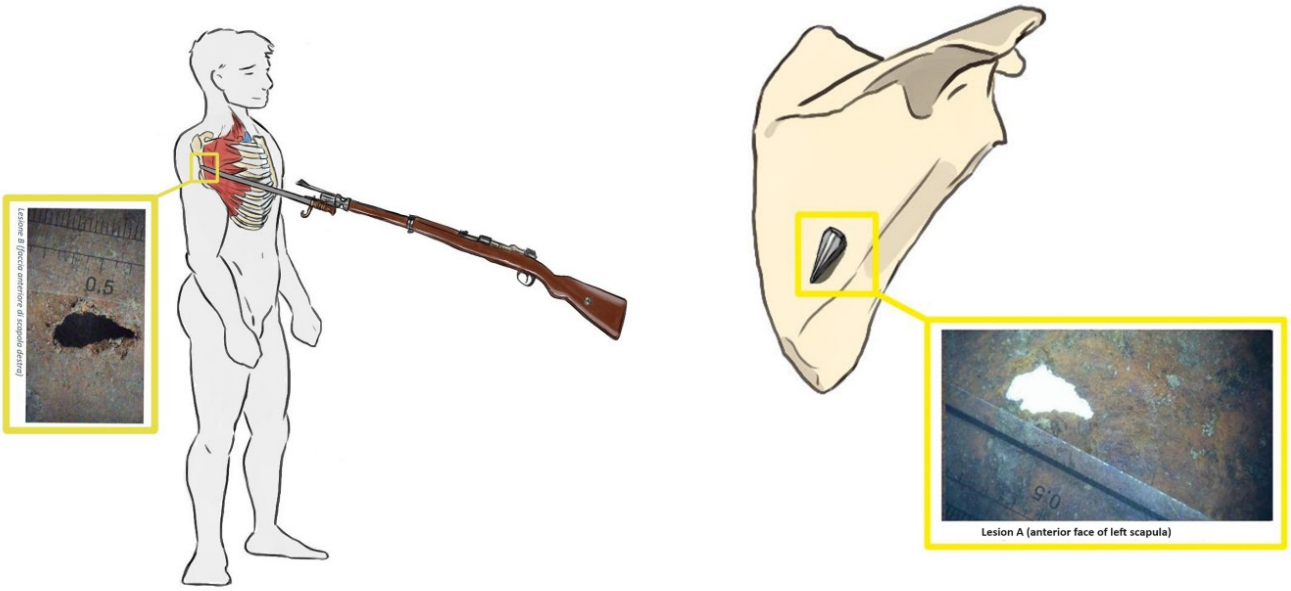

articulated from the ipsilateral upper limb at the level of the ulna-carpal girdle.

The presence of a few and limited fractures of the bone structures of the wrist can lead to the intervention of a weapon such as a "slash" (axe, hatchet, etc.). This type of weapon combines the characteristics of a high weight, typical of blunt instruments made of cohesive material with high density, with those of the cutting action of a wire. Therefore, it is suitable for determining the complete disarticulation of the district with just a few blows inflicted.

In conclusion, it is possible that C2 was the victim of an assault in which his left hand was amputated, he was beaten and pierced at least twice by a bayonet, and finally, he was killed with a rifle shot to the head. It seems reasonable to assume that a gunshot wound caused the extensive sphelative-fracture complex with greater interest in the left part of the skull. Also, further injuries are to be reported, in particular the two continuous solutions of the right scapular plate, referable to the action of a point and cut cold weapon, such as the tip of a bayonet, acting from front to back and piercing the chest, which could have caused, in any case, visceral lesions or even vascular sections, even of significant causative entities of acute pathological situation such for example pneumothorax or secondary hemothorax and vascular section. Nonetheless, we must consider the results of the amputation of the left hand, probably carried out using a slashing blade weapon, therefore very heavy, and capable of thoroughly dissecting the wrist with one or at least a few blows inflicted. The reconstruction of the lethal trauma dynamics allows to identify those peculiar characteristics in the killing of a man with violence and ferocity, represented by the plurality of harmful methods of attacking the body of the victim (firearm and bladed weapon) and from the implementation of harmful paintings of violation of its integrity (left hand amputation).

Conclusion

The present paper aims to discuss the recovery and study of human remains in the Chapel of St. Dominic of the Cathedral of 'Al-Tahira' in Qaraqosh (Iraq) in 2022.

A team of Italian forensic anthropologists and pathologists were involved in the excavations, which allowed the discovery of skeletal remains referred to as two individuals (here named C1 and C2). Each bone remains was examined, inferring information about sex estimation, height calculation, age at death calculation, and dental formula. Bone elements underwent microscopic examination. Both anatomically repositioned bone remains were subjected to CT examination, and facial reconstructions were performed. Finally, the cause and manner of death were hypothesised.

An extensive fracture complex with transverse orientation was observed in the occipital region of C1. C2 showed cranial disintegration, with fracture fragments affecting the structures of the left neuro- and splanchnic skull, and to a greater extent, the left hemifacial, orbital, and zygomatic regions and the same side of the face. In addition, no bones attributable to the left hand of C2 were found.

Regarding C1, the findings are consistent with death caused by severe blunt-force trauma, particularly affecting the cranial region. On the other hand, it seems reasonable to assume that C2 was the victim of an assault in which his left hand was amputated, he was beaten and pierced by a bayonet, and finally, he was killed with a rifle shot to the head.

References

Acsádi, G., & Nemeskéri, J. (1970). *History of human life span and mortality.* Akadémiai Kiadó.

Baca, K., Bridge, B., & Snow, M. (2022). *Three-dimensional geometric morphometric sex determination of the whole and modeled fragmentary human pubic bone.* PLoS One, 6;17(4):e0265754. https://doi.org/10.1371/journal.pone.0265754.

Ball, R. (2011). *Mauser Military Rifles of the Word.* Gun Digest Books.

Crudele, G.D.L., Merelli, V.G., Vener, C., Milani, S., Cattaneo, C. (2020). *The Frequency of Cranial Base Fractures in Lethal Head Trauma.* J Forensic Sci, 65(1):193-195. https://doi.org/10.1111/1556-4029.14149.

Convention against Torture and other Cruel, Inhuman or Degrading Treatment or Punishment and Optional Protocol to the Convention against Torture and other Cruel, Inhuman or Degrading Treatment or Punishment. (1984). https://cti2024.org/resource/un-convention-against-torture-and-other-cruel-inhuman-or-degrading-treatment-or-punishment-and-the-optional-protocol/

Christensen, A.M., Passalacqua, N.V., Bartelink, E.J. (2019). *Forensic Anthropology.* Academic Press.

Donato, L., Ubelaker, D.H., Marsella, L.T., Bugelli, V., Camatti, J., Treglia, M., Cecchi, R. (2024). *Applications of forensic anthropology methodology: accuracy of virtual face reproductions performed on the Tenchini collection.* Forensic Sci Med Pathol. https://doi.org/10.1007/s12024-024-00839-y.

Haug, R.H., Adams, J.M., Conforti, P.J., Likavec, M.J. (1994). *Cranial fractures associated with facial fractures: a review of mechanism, type, and severity of injury*. J Oral Maxillofac Surg, 52(7):729-33. https://doi.org/10.1016/0278-2391(94)90488-x.

Işcan, M.Y., & Steyn, M. (2013). *The Human Skeleton in Forensic Medicine*. Charles C. Thomas. Klepinger, L.L. (2006). *Fundamentals of Forensic Anthropology*. Wiley-Liss.

Lee, H., Podaras, N., Nikita, E., Chovalopoulou, M.E., Garoufi, N. (2024). *Stature estimation equations from fragmentary long bones based on a modern Eastern Mediterranean assemblage.* Anthropol

Anz. https://10.1127/anthranz/2024/1850.

Lovejoy, C.O., Meindl, R., Pryzbeck, T.R., Mensforth, R.P. (1985). *Chronological metamorphosis of the auricular surface of the ilium: a new method for the determination of adult skeletal age at death.* Am J Phys Anthropol, 68:15–28.

Ost, A.M. (2022). *Age-at-death estimation from the auricular surface of the ilium: A test of a sex-specific component method.* J Forensic Sci, 67(3):868-876. https://doi.org/10.1111/1556-4029.14983.

Madea, B. (2014). *Germany – Handbook of Forensic Medicine.* Wiley Blackwell.

Sahoo, D., Deck, C., Yoganandan, N., Willinger, R. (2013). *Anisotropic composite human skull model and skull fracture validation against temporo-parietal skull fracture.* J Mech Behav Biomed Mater, 28:340-53. https://doi.org/10.1016/j.jmbbm.2013.08.010.

Sahoo, D., Deck, C., Yoganandan, N., Willinger, R. (2016). *Development of skull fracture criterion based on real-world head trauma simulations using finite element head model.* J Mech Behav Biomed Mater, 57:24-41. https://doi.org/10.1016/j.jmbbm.2015.11.014.

Simon, L.V., & Newton, E.J. (2024). *Basilar Skull Fractures.* https://www.ncbi.nlm.nih.gov/books/NBK470175/

Todd, T.W. (1920). *Age changes in the pubic bone. I. The male White pubis.* Am J Phys Anthropol, 3:285–334.

Trotter, M. (1970). Estimation of stature from intact long limb bones. In Stewart, T.D. (Ed.). *Personal Identification in Mass Disasters: National Museum of Natural History.* Washington.

White T., & Folkens, P. A. (2005). *The human bone manual*. CRC press.

Yoganandan, N., & Pintar, F.A. (2004). *Biomechanics of temporo-parietal skull fracture*. Clin Biomech (Bristol, Avon), 19(3):225-39. doi: https://doi.org/10.1016/j.clinbiomech.2003.12.014.

Submitted 4th of Oct. 2024
Accepted 29th of Apr 2025